

Adhesion of polymers to electrodeposited copper for a new 3D printing technology for metal-polymer hybrid components

Dawid Kiesiewicz^{1,2} , Maciej Pilch^{2*} , Bartosz Oksiuta¹ , Justyna Pawlik³

¹ Cracow University of Technology, Faculty of Chemical Engineering and Technology, Department of Biotechnology and Physical Chemistry, Warszawska 24, 31-155 Cracow, Poland

² Cracow University of Technology, Faculty of Civil Engineering, Wind Engineering Laboratory, Warszawska 24, 31-155 Cracow, Poland

³ AGH University of Science and Technology, Faculty of Materials Science and Ceramics, Al. Mickiewicza 30, 30-059 Cracow, Poland

* Corresponding author, e-mail:
maciej.pilch@pk.edu.pl

Presented at
4rd Seminar on Practical Aspects
of Chemical Engineering PAIC 2024,
16–17 May 2024, Zaniemyśl, Poland.
Guest Editors: Andżelika Krupińska
and Sylwia Włodarczak.

Article info:

Received: 20 July 2024

Revised: 23 October 2024

Accepted: 21 November 2024

Abstract

3D printing has significantly evolved in recent years. Initially, only plastics were used as materials for 3D printing, but technological advancement has enabled 3D printing with materials such as metals, ceramics and biomaterials. With the development of 3D printing, there emerged a need to create a printer for producing hybrid parts, such as metal-plastic, characterized by both the exceptional strength and durability of metal and the lightweight and insulating properties of plastics. The new technique of 3D printing involves layer-by-layer metal growth in the electroplating process, as well as extrusion of a photopolymer composition, followed by UV light curing on the surface of a copper layer. Prints from this new type of 3D printer must exhibit strong adhesive bonding to prevent damage to the printed model. Therefore, mechanical tests were conducted to examine the adhesion of prepared photopolymer compositions to copper sheet coated with electroplated metal and to regular copper sheet in order to compare the obtained values. Analyzing the test results, it can be concluded that the structure of electrodeposited copper significantly improves the adhesive bond strength.

Keywords

adhesion, photopolymerization, electrodeposition, 3D printing, hybrid components

1. INTRODUCTION

The adhesion of polymers to metals is crucial in many technical applications such as the automotive, aerospace, medical, defense, and electronics industries (Grujicic et al., 2008; Rahme et al., 2011; Trzepieciński et al., 2021; Zhao et al., 2007). The use of polymer materials is becoming increasingly common due to their low weight and insulating properties. (Campilho et al., 2018) Adhesion strength values have been determined for a limited number of polymer materials (such as acrylates and epoxies) to several metals because various physical and chemical phenomena can occur during interface formation (Fug et al., 2017; Nies et al., 2014; Patel et al., 2009).

Polymer-to-metal adhesion can be enhanced through various mechanisms, such as wettability, the addition of chemical groups, and surface topography modification (Hamdi et al., 2020; Neagu and Neagu, 1993; Schuberth et al., 2016). Improving wettability involves increasing the polymer's ability to spread evenly over the metal surface, thereby increasing the contact area and strengthening the bond. Adding chemical groups, such as polar groups, allows for the formation of chemical bonds between the polymer and the metal. Modifying surface topography, for example through mechanical or chemical treatment, increases the contact surface area, resulting in higher adhesive bonding strength (Evans et al., 2002; Kaneko et al., 2005; Ochoa-Putman and Vaidya, 2011).

Studies on adhesion between metals and polymers can be conducted using spectroscopic techniques (XPS, FTIR, IETS, SIMS, and quantum mechanics modeling) (Fug et al., 2014; Nies et al., 2014), as well as mechanical tests on two types of samples: sandwich-type and bimaterial. Sandwich-type samples are constructed by joining a coating with two halves of the substrate material, where the coating thickness is very small compared to the crack length and other length scales of the sample. Therefore, most of the sample is homogeneous, except for the thin coating layer (Alphonse et al., 2021; Ramnath et al., 2019) For homogeneous material, classical fracture mechanics is used. Several solutions already exist to evaluate fracture toughness or the strain energy release rate. Since the coating in a sandwich sample is relatively thin, complications due to the inhomogeneity introduced by this thin coating are usually neglected. Therefore, it is common practice to use the fracture toughness or strain energy release rate determined for a homogeneous sample without coating to characterize interfacial fracture in the presence of a coating. Typical techniques used for testing these types of samples include Double Cantilever Beam, four-point bend, brazil-nut, and double cleavage drilled compression (Chen et al., 2014; Hutchinson and Suo, 1991; Maassen et al., 2021; Suo and Hutchinson, 1989). The other type are bimaterial samples, which are relatively easy to manufacture



and can provide good qualitative or quantitative information. Furthermore, evaluating coating adhesion using bimaterial samples usually does not require attaching new devices to the coating. Examples of measurement methods using bimaterial samples include indentation test, scratch test, peel test, and blister test (Lesage and Chicot, 1999; Marot et al., 2006; Suo and Hutchinson, 1989).

This research focused on the influence of the metal part's surface on adhesive bonding strength for the development of a new 3D printing technology for metal-polymer hybrid components. The new 3D printing technique utilizes two processes: metal electrodeposition and acrylate resin photopolymerization. Therefore, studies were conducted on the adhesive bonding strength of acrylate and urethane-acrylate resins to both plain copper sheet and copper sheet coated with electrodeposited copper.

2. EXPERIMENTAL PART

2.1. Chemical substances

For the role of monomers in the photocurable compositions analyzed in this study, acrylate monomers and their mixtures were selected, such as: 2,2-bis[4(2-hydroxy-3-methacryloxypropoxy)phenyl]propane (Bis-GMA) from Sigma-Aldrich, EBECRYL 45 (E45), a tetrafunctional acrylated oligomer from Allnex, EBECRYL 130 (E130), an aliphatic diacrylate from Allnex, EBECRYL 285 (E285), an aliphatic urethane diacrylate oligomer diluted 25% with tripropylene glycol diacrylate from Allnex, EBECRYL 3300 (E3300), a modified bisphenol-A-based epoxy acrylate oligomer from Allnex, EBECRYL 4740 (E4740), an aliphatic urethane acrylate from Allnex, and EBECRYL 4858 (E4858), an aliphatic urethane diacrylate from Allnex.

Diphenyl(2,4,6-trimethylbenzoyl)phosphine oxide (TPO) from Allnex was used as the photoinitiator.

For preparing the electroplating baths, copper(II) sulfate pentahydrate from Sigma-Aldrich and sulfuric acid (VI) with a concentration of 98% from Warchem were used.

2.2. Sample Preparation

2.2.1. Photocurable Compositions

As part of the study, six photocurable compositions were prepared. Three of them consisted of a single monomer (E285, E4740, E4858), and three consisted of two comonomers in equal concentrations (E45+BisGMA, E130+BisGMA, E3300+BisGMA). A photoinitiator, TPO, was added to each composition at a ratio of 1% of the total sample mass.

2.2.2. SEM/EDS Materials Characteristics

Surface topography studies using a scanning electron microscope coupled with an EDS detector were conducted on both the cross-section and the top surface of the sample. For this purpose, a small fragment was cut from the sample using metal shears and attached to a special disk with carbon tape. The disk was then placed in the microscope chamber, and the examination began.

The quality of the resulting layer was assessed based on the surface of the metal produced through the electrolysis process. To determine the thickness of the sample, AutoCAD was used, where the exact layer thickness value was assessed based on the length of lines applied to the sample thickness and to a ruler that was placed in each microscope image.

2.2.3. Mechanical Strength Tests

Strength tests were carried out on paddle-type samples (Figure 1). The preparation of the paddles for testing the adhesion of resin to metal began with creating a computer model of the fitting in the Fusion 360 software (Autodesk). The dimensions of the fitting are shown in Figure 1.

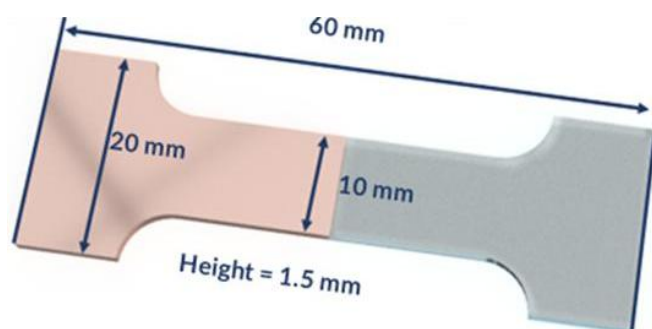


Figure 1. Visualization of the paddle for adhesion testing along with dimensions.

The fitting consists of two materials. One half was made of copper and the other from a photo-curable composite. To achieve the desired shape, a mold was printed on an Anycubic Photon Mono X 6K 3D printer using commercially available Anycubic Standard Clear resin, which was then filled with Progmar two-component silicone for molds (Figure 2).

The copper fittings were cut from 1.5 mm thick copper sheet using a CNC laser cutter. Then, half of them underwent an electrodeposition process in a saturated copper sulfate solution with one molar sulfuric acid. This process was conducted at 2 V for 10 minutes. Next, the sheet was placed in a silicone mold and the other half was filled with a photocurable composite. The resin polymerization process was carried out for 10 minutes using a UV diode with a wavelength of $\lambda_{\max} = 365 \text{ nm}$ at an intensity of $87.8 \text{ mW}\cdot\text{cm}^{-2}$ (light intensity was measured using a PM160 power meter with a Si

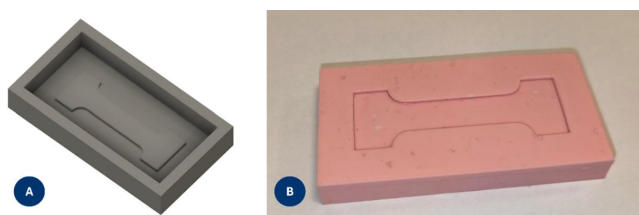


Figure 2. Model designed in Fusion 360 for casting a silicone mold (A) and finished mold for preparing two-material paddles (B).

Sensor from Thorlabs). Six fittings were made for each selected photo-curable composite. Three of them were prepared using standard copper sheet (99.99% purity), while the other three were made using copper sheet additionally coated with a layer of copper through the electrodeposition process.

2.3. Apparatus

The samples were subjected to a static tensile test, using a stretching rate of 10 mm/min and a preload force of 1 N. These parameters remained constant for all the tested materials. Three samples were prepared for each type of material. The tested sample was gripped at both ends with clamps, and the measurement began, which involved stretching the sample until the adhesive bond broke. As a result of the tests, values for Young's modulus (E [MPa]), tensile strength (σ_M [MPa]), and the maximum force at which the sample failed (F_{max} [N]) were obtained.

Microscopic surface topography analysis of the electrodeposited metal was performed using a Hitachi S-4700 field emission scanning electron microscope (FE SEM).

3. RESULTS

3.1. Materials Characteristics

Since the photopolymerization process of the analyzed monomers is well-known and has been previously studied, only a visual inspection was conducted to identify potential structural defects in the polymer parts of the prepared samples (Mucci et al., 2009; Tehfe et al., 2013; Tomal et al., 2024). A sample image of one of the specimens with marked structural defects is shown in Figure 3.

In most of the analyzed samples, small structural defects in the form of air bubbles trapped within the polymer structure were observed. These defects likely resulted from the high speed of the polymerization process and reduced the mechanical strength of the polymer parts of the hybrid details. Based on this observation, it was concluded that during the strength

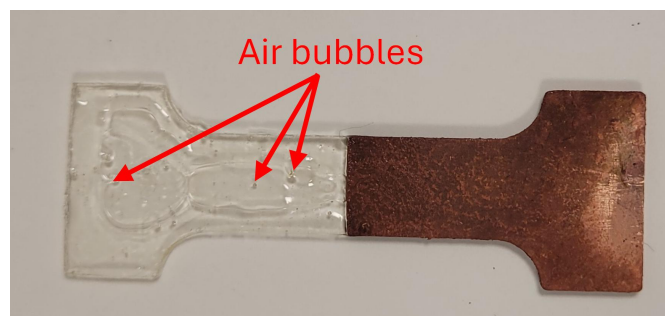


Figure 3. Image of a hybrid detail sample for adhesion strength testing at the metal-polymer interface.

tests of the hybrid details, the samples should be carefully observed to detect any potential breakage in the polymer part's structure, as this could lead to results with significant errors.

Analyzing the SEM images of the examined samples, it can be concluded that they are characterized by a fine-grained, dense metal structure, indicating a properly conducted electroplating process. At the same time, it is easy to notice that the metal surface is not smooth, as in the case of samples cut from copper sheet, but slightly porous, which may increase the adhesive force at the metal-polymer interface in hybrid details. The increase in this adhesive force is due to the increased contact area between the metal and the polymer resulting from the porous structure. An example SEM image of a fragment of the metal (copper) part of the hybrid detail is shown in Figure 4.

Based on the analysis of EDS spectra for the studied samples, it was determined that the average mass content of metallic copper in the samples was approximately 92.8%, and the oxygen content was around 3.8%. The EDS spectrum of sample E285 is shown in Figure 5.

In the EDS spectra of some samples, small signals from elements such as carbon, sulfur, and iron can also be observed. The carbon likely originates from the carbon tape used. Sulfur may have entered the sample from the electroplating bath solution. Trace amounts of iron could have been introduced to the sample during cutting with steel shears. Based on the obtained data, it can be concluded that the sample E285 contains the highest number of metallic copper atoms (94.35% copper mass content). The mass and atom contents of copper and oxygen in the analyzed samples are summarized in Table 1. The copper content by mass for each sample is above 90.0%. This proves that the copper layers produced on the analyzed samples using the electrodeposition technique consist mainly of metallic copper with a small amount of oxides. The composition of the electrodeposited copper layers obtained can be compared with the composition of sample electrodeposited copper layers from the literature (Soegjono et al., 2020). In this case, only signals originating from copper and oxygen were observed. As can be seen, the composition of electrodeposited metal layers strongly depends on the composition of the electroplating baths and the sample preparation methods used.

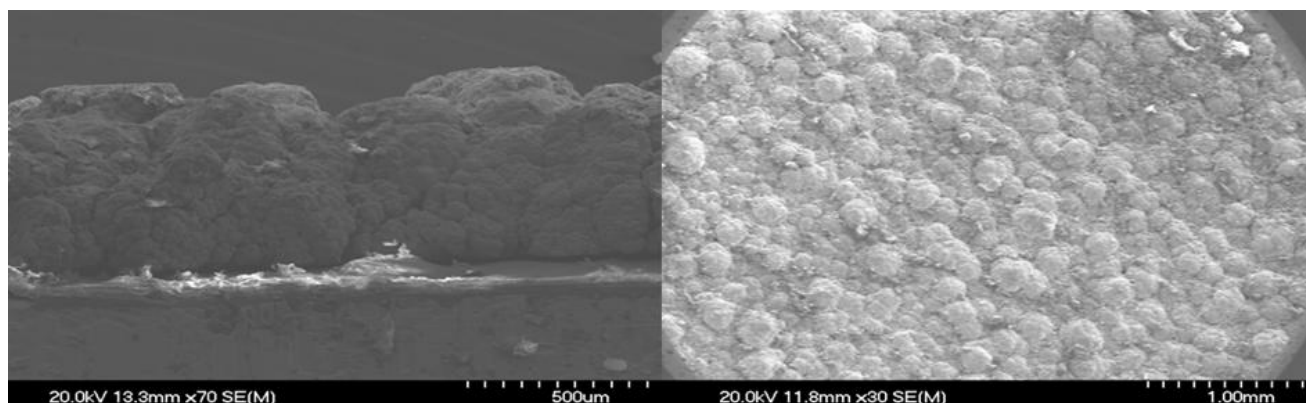


Figure 4. Image of a hybrid detail sample for adhesion strength testing at the metal-polymer interface.

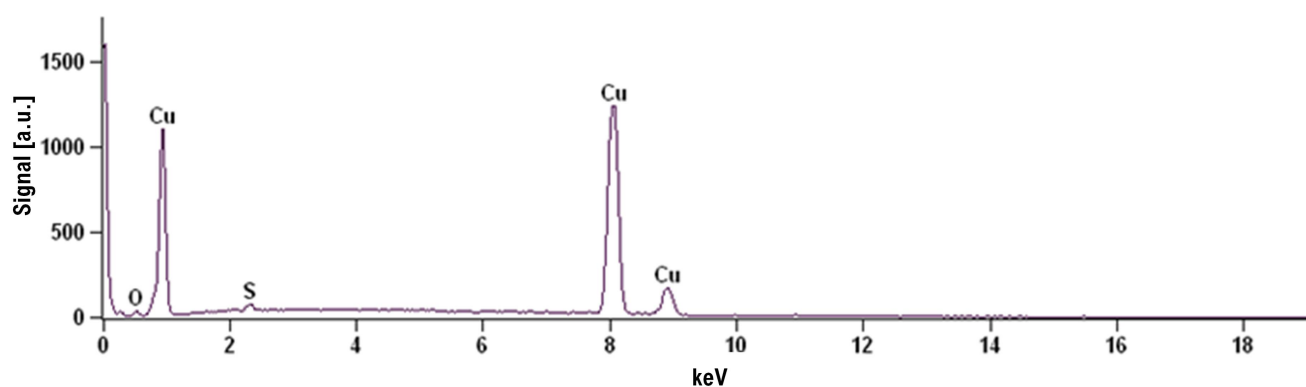


Figure 5. EDS spectrum of E285 sample (electrodeposited layer).

Table 1. Mass and atom contents of copper and oxygen in the analyzed samples.

Sample name	E285	E3300+ BisGMA	E4740	E4858	E130+ BisGMA	E45+ BisGMA
Copper mass content [%]	94.35	90.85	92.57	93.25	92.98	92.64
Oxygen mass content [%]	2.70	4.79	3.45	3.81	3.48	4.32
Copper atom content [%]	85.02	76.66	81.09	81.65	81.69	79.91
Oxygen atom content [%]	9.65	16.05	11.99	13.24	12.14	14.79

3.2. Mechanical Strength Tests

During the measurement for samples made of copper and the polymer based on the E4858 composition, the adhesive bond ruptured while placing the sample on the measurement stand. This was due to excessive bending of the sample that occurred during the photocuring of the E4858 composition. Similarly, one sample made from the E130+BisGMA composition was destroyed. In the case of one sample based on the E45+BisGMA composition, the polymer part of the sample was damaged during the measurement. The summary of the mechanical strength test results is presented in Table 2.

The adhesion assessment was based on the maximum force at which the sample failed (F_{\max}). The F_{\max} values were higher for samples with copper sheets coated with a layer of elec-

troplated copper. This is due to the greater contact surface. The electroplated copper had a granular structure, while the ordinary copper sheet had a flat surface. The highest F_{\max} values were characterized by samples made from light-curable compositions named E3300+BisGMA, E4740, E4858, and E130+BisGMA. These values were obtained for a small contact surface area of 0.15 cm². These compositions enable the formation of a durable adhesive bond with electroplated copper and may find applications in the 3D printing of hybrid parts. Tensile strength values, similarly to the maximum force at which the sample failed, improved for samples with a layer of electroplated copper. This is also due to the greater contact surface at the metal-plastic interface. Analyzing the Young's modulus values for all the samples made, no correlation was found between the type of sample and the modulus value. This may be due to the samples having slight deformations

Table 2. Results of strength tests (average of 3 samples).

Sample name	Sample type	E [MPa]	σM [MPa]	F_{max} [N]
E285	Copper plate	9.50	0.11	1.71
	Electrodeposited layer	386.00	5.47	82.10
E3300+BisGMA	Copper plate	224.67	10.35	155.26
	Electrodeposited layer	60.67	12.37	185.62
E4740	Copper plate	238.67	2.70	40.57
	Electrodeposited layer	34.67	8.31	124.63
E4858	Copper plate	–	–	–
	Electrodeposited layer	96.67	10.45	156.72
E130+BisGMA	Copper plate	2.50	4.98	74.72
	Electrodeposited layer	199.00	9.87	148.07
E45+BisGMA	Copper plate	137.00	1.56	23.40
	Electrodeposited layer	50.00	5.96	89.44

that occurred during the photopolymerization process of the light-curable compositions. For comparison, the results of similar studies on polymer-metal joints can be found in the literature (Kafkopoulos et al., 2021; Melentiev et al., 2023). However, the tests presented in this paper were conducted specifically with the aim of developing a 3D printing technique using the electrodeposition process with dedicated equipment for this purpose, which makes them unique and allows for predicting the properties of hybrid metal-polymer parts produced using this 3D printing technique. Although the literature describes studies on the adhesion of metals to polymers, adhesion to thermoplastics is usually considered. There are also studies on the adhesion of metals to photopolymerizable compositions. However, these studies take a completely different form than those described in this work. There is no mention in the literature of the investigation of the metal-polymer adhesive bond in hybrid parts produced using the technique described in this paper, which has been employed in the ongoing development of a multi-material 3D printer capable of producing such parts in a single 3D printing process (Augustyn et al., 2021; Golaz et al., 2013).

4. Conclusions

Samples used for strength testing made from copper sheet coated with electroplated copper showed higher values of tensile strength and maximum force at which the sample failed compared to samples made from ordinary copper sheet. This is due to increased porosity in samples coated with electroplated copper compared to those made from plain copper sheet, which results in a larger contact area between the metal and the polymer in the electroplated samples (Figure 6). This suggests that the proposed combination of photopolymerization and electroplating techniques could enable the production of hybrid 3D-printed metal-polymer details with strength of the metal-polymer interface that is unachievable with other

manufacturing methods. The samples with the highest F_{max} values were characterized by light-curable compositions named E3300+BisGMA, E4740, E4858, and E130+BisGMA.

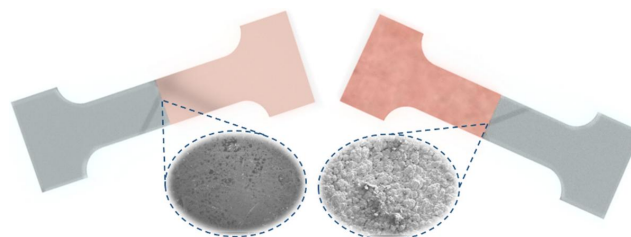


Figure 6. Visualization of a paddle made from plain copper sheet (left) and copper sheet with electroplated copper layer (right).

Acknowledgements

The research work was conducted as part of the LIDER XII project (agreement no. LIDER/51/0270/L-12/20/NCBR/2021) titled „Multi-material 3D printer dedicated to production of solid metal and galvanic alloys parts, as well as metal-polymer hybrid elements using developed coupled technology of metal electrodeposition and photopolymerization of polymer resins” funded by the National Centre for Research and Development.

REFERENCES

- Alphonse M., Bupesh Raja V.K., Gopala Krishna V., Kiran R.S.U., Venkata Subbaiah B., Vinay Rama Chandra L., 2021. Mechanical behavior of sandwich structures with varying core material – A review. *Mater. Today: Proc.*, 44, 3751–3759. DOI: [10.1016/j.matpr.2020.11.722](https://doi.org/10.1016/j.matpr.2020.11.722).
- Augustyn P., Rytlewski P., Moraczewski K., Mazurkiewicz A., 2021. A review on the direct electroplating of polymeric materials. *J. Mater. Sci.*, 56, 14881–14899. DOI: [10.1007/s10853-021-06246-w](https://doi.org/10.1007/s10853-021-06246-w).

- Campilho R.D.S.G., da Silva L.F.M., Banea M.D., 2018. Adhesive bonding of polymer composites to lightweight metals. In: Amancio-Filho S.T., Blaga L.A. (Eds.), *Joining of polymer-metal hybrid structures*. John Wiley & Sons Inc., 29–59. DOI: [10.1002/9781119429807.ch2](https://doi.org/10.1002/9781119429807.ch2).
- Chen Z., Zhou K., Lu X., Lam Y. C., 2014. A review on the mechanical methods for evaluating coating adhesion. *Acta Mech.*, 225, 431–452. DOI: [10.1007/s00707-013-0979-y](https://doi.org/10.1007/s00707-013-0979-y).
- Evans R.D., Doll G.L., Morrison Jr. P.W., Bentley J., More K.L., Glass J.T., 2002. The effects of structure, composition, and chemical bonding on the mechanical properties of Si-C:H thin films. *Surf. Coat. Technol.*, 157, 197–206. DOI: [10.1016/S0257-8972\(02\)00164-0](https://doi.org/10.1016/S0257-8972(02)00164-0).
- Fug F., Nies C., Possart W., 2014. *In situ* FTIR study of adhesive interactions of 4,4'-methylene diphenyl diisocyanate and native metals. *Int. J. Adhes. Adhes.*, 52, 66–76. DOI: [10.1016/j.ijadhadh.2014.04.004](https://doi.org/10.1016/j.ijadhadh.2014.04.004).
- Fug F., Petry A., Jost H., Ahmed A., Zamanzade M., Possart W., 2017. Molecular layer deposition of polyurethane – polymerisation at the very contact to native aluminium and copper. *Appl. Surf. Sci.*, 426, 133–147. DOI: [10.1016/j.apsusc.2017.07.177](https://doi.org/10.1016/j.apsusc.2017.07.177).
- Golaz B., Michaud V., Manson J.-A.E., 2013. Photo-polymerized epoxy primer for adhesion improvement at thermoplastics/metallic wires interfaces. *Composites, Part A: Appl. Sci. Manuf.*, 48, 171–180. DOI: [10.1016/j.compositesa.2013.01.017](https://doi.org/10.1016/j.compositesa.2013.01.017).
- Grujicic M., Sellappan V., Omar M.A., Seyr N., Obieglo A., Erdmann M., Holzleitner J., 2008. An overview of the polymer-to-metal direct-adhesion hybrid technologies for load-bearing automotive components. *J. Mater. Process. Technol.*, 197, 363–373. DOI: [10.1016/j.jmatprotec.2007.06.058](https://doi.org/10.1016/j.jmatprotec.2007.06.058).
- Hamdi M., Saleh M.N., Poulis J.A., 2020. Improving the adhesion strength of polymers: effect of surface treatments. *J. Adhes. Sci. Technol.*, 34, 1853–1870. DOI: [10.1080/01694243.2020.1732750](https://doi.org/10.1080/01694243.2020.1732750).
- Hutchinson J.W., Suo Z., 1991. Mixed mode cracking in layered materials. *Adv. Appl. Mech.*, 29, 63–191. DOI: [10.1016/S0065-2156\(08\)70164-9](https://doi.org/10.1016/S0065-2156(08)70164-9).
- Kafkopoulos G., Padberg C.J., Duvigneau J., Vancso G.J., 2021. Adhesion engineering in polymer–metal comolded joints with biomimetic polydopamine. *ACS Appl. Mater. Interfaces*, 13, 19244–19253. DOI: [10.1021/acsmi.1c01070](https://doi.org/10.1021/acsmi.1c01070).
- Kaneko T., Nemoto D., Horiguchi A., Miyakawa N., 2005. FTIR analysis of a SiC:H films grown by plasma enhanced CVD. *J. Cryst. Growth*, 275, e1097–e1101. DOI: [10.1016/j.jcrysgro.2004.11.128](https://doi.org/10.1016/j.jcrysgro.2004.11.128).
- Lesage J., Chicot D., 1999. Models for hardness and adhesion of coatings. *Surf. Eng.*, 15, 447–453. DOI: [10.1179/026708499101516821](https://doi.org/10.1179/026708499101516821).
- Maassen S.F., Erdle H., Pulvermacher S., Brands D., Böhlke T., Gibmeier J., Schröder J., 2021. Numerical characterization of residual stresses in a four-point-bending experiment of textured duplex stainless steel. *Arch. Appl. Mech.*, 91, 3541–3555. DOI: [10.1007/s00419-021-01931-3](https://doi.org/10.1007/s00419-021-01931-3).
- Marot G., Lesage J., Démarécaux P., Hadad M., Siegmans S., Staia M.H., 2006. Interfacial indentation and shear tests to determine the adhesion of thermal spray coatings. *Surf. Coat. Technol.*, 201, 2080–2085. DOI: [10.1016/j.surfcoat.2006.04.046](https://doi.org/10.1016/j.surfcoat.2006.04.046).
- Melentiev R., Tao R., Fatta L., Tevtia A.K., Verghese N., Lubineau G., 2023. Towards decoupling chemical and mechanical adhesion at the electroplated metal/polymer interface via precision surface texturing. *Surf. Interfaces*, 38, 102875. DOI: [10.1016/j.surfin.2023.102875](https://doi.org/10.1016/j.surfin.2023.102875).
- Mucci V., Arenas G., Duchowicz R., Cook W.D., Vallo C., 2009. Influence of thermal expansion on shrinkage during photopolymerization of dental resins based on bis-GMA/TEGDMA. *Dent. Mater.*, 25, 103–114. DOI: [10.1016/j.dental.2008.04.014](https://doi.org/10.1016/j.dental.2008.04.014).
- Neagu E., Neagu R., 1993. Polymer surface treatment for improvement of metal-polymer adhesion. *Appl. Surf. Sci.*, 64, 231–234. DOI: [10.1016/0169-4332\(93\)90029-B](https://doi.org/10.1016/0169-4332(93)90029-B).
- Nies C., Fug F., Otto C., Possart W., 2014. Adhesion of polyurethanes on native metal surfaces – stability and the role of urea-like species. *Int. J. Adhes. Adhes.*, 52, 19–25. DOI: [10.1016/j.ijadhadh.2014.03.006](https://doi.org/10.1016/j.ijadhadh.2014.03.006).
- Ochoa-Putman C., Vaidya U.K., 2011. Mechanisms of interfacial adhesion in metal–polymer composites – effect of chemical treatment. *Composites, Part A: Appl. Sci. Manuf.*, 42, 906–915. DOI: [10.1016/j.compositesa.2011.03.019](https://doi.org/10.1016/j.compositesa.2011.03.019).
- Patel R.M., Shukla M.J., Patel K.N., Patel H.K., 2009. Biomaterial based novel polyurethane adhesives for wood to wood and metal to metal bonding. *Mater. Res.*, 12, 385–393. DOI: [10.1590/S1516-14392009000400003](https://doi.org/10.1590/S1516-14392009000400003).
- Rahme R., Avril F., Cassagnau P., Sage D., Verchère D., Doux M., 2011. New polymer/steel solution for automotive applications. *Int. J. Adhes. Adhes.*, 31, 725–734. DOI: [10.1016/j.ijadhadh.2011.06.015](https://doi.org/10.1016/j.ijadhadh.2011.06.015).
- Ramnath B.V., Alagarraja K., Elanchezian C., 2019. Review on sandwich composite and their applications. *Mater. Today Proc.*, 16, 859–864. DOI: [10.1016/j.matpr.2019.05.169](https://doi.org/10.1016/j.matpr.2019.05.169).
- Schuberth A., Göring M., Lindner T., Töberling G., Puschmann M., Riedel F., Scharf I., Schreiter K., Spange S., Lampke T., 2016. Effect of new adhesion promoter and mechanical interlocking on bonding strength in metal-polymer composites. *IOP Conf. Ser.: Mater. Sci. Eng.*, 118, 012041. DOI: [10.1088/1757-899X/118/1/012041](https://doi.org/10.1088/1757-899X/118/1/012041).
- Soegijono B., Susetyo F.B., Situmorang E.U.M., Yusmaniar, 2020. Effect of current density on crystallographic orientation, and oxidation behavior of copper plated on aluminum substrate. *Asian J. Appl. Sci.*, 8, 200–207. DOI: [10.24203/ajas.v8i4.6287](https://doi.org/10.24203/ajas.v8i4.6287).
- Suo Z., Hutchinson J.W., 1989. Sandwich test specimens for measuring interface crack toughness. *Mater. Sci. Eng. A*, 107, 135–143. DOI: [10.1016/0921-5093\(89\)90382-1](https://doi.org/10.1016/0921-5093(89)90382-1).
- Tehfe M.A., Louradour F., Lalevée J., Fouassier J.-P., 2013. Photopolymerization reactions: on the way to a green and sustainable chemistry. *Appl. Sci.*, 3, 490–514. DOI: [10.3390/app3020490](https://doi.org/10.3390/app3020490).

Tomal W., Gałuszka K., Lepcio P., Pilch M., Chachaj-Brekiesz A., Korčušková M., Ortyl J., 2024. Naphthalene–stilbenes as effective visible-light sensitizers to study the effect of diluent and nanofillers on *in situ* photopolymerization and 3D-VAT printing process. *Mater. Adv.*, 5, 788–805. DOI: [10.1039/D3MA00943B](https://doi.org/10.1039/D3MA00943B).

Trzepieciński T., Najm S.M., Sbayti M., Belhadjsalah H., Szpunar M., Lemu H.G., 2021. New advances and future possibilities in forming technology of hybrid metal–polymer composites used in aerospace applications. *J. Compos. Sci.*, 5, 217. DOI: [10.3390/jcs5080217](https://doi.org/10.3390/jcs5080217).

Zhao Q., Wang C., Liu Y., Wang S., 2007. Bacterial adhesion on the metal-polymer composite coatings. *Int. J. Adhes. Adhes.*, 27, 85–91. DOI: [10.1016/j.ijadhadh.2006.01.001](https://doi.org/10.1016/j.ijadhadh.2006.01.001).